Lab on a Chip

PAPER

View Article Online
View Journal | View Issue

Cite this: *Lab Chip*, 2025, **25**, 5482

Interplay between dietary fiber, macrophages and colonocytes in a microfluidic model of host-microbiota interactions in colorectal cancer

Daniel Penarete-Acosta, †[a] Mohet Mittal,†[b] Sanjukta Chakraborty,[c] Arum Han [abd] and Arul Jayaraman*[ab]

Dietary fiber has been consistently associated with a decreased risk of colorectal cancer development. While the apoptotic effect of dietary fiber microbial fermentation products, such as short chain fatty acids on tumor colonocytes, is well established, the role of these products on other components of the tumor microenvironment remains unexplored. Tumor associated macrophages play a critical role in tumor development in colorectal cancer; however, the effect of dietary fiber fermentation by microbiota on the interaction between macrophages and colonocytes in the colorectal cancer microenvironment has been difficult to dissect due to a lack of *in vitro* models of colorectal cancer containing immune cells, colonocytes, and microbiota. Recently, we developed a microfluidic model that facilitates the coculture of colorectal cancer spheroids with complex microbial communities. Here, we expand our model to include macrophages and employ it to study the impact of dietary fiber on macrophage-colonocyte interaction. We optimized monocyte differentiation parameters *in vitro* and demonstrated the capacity of our model to recapitulate changes in microbiota composition and metabolic output associated with dietary fiber administration *in vivo*. Coculture of colonocytes with microbiota and macrophages revealed that alterations in microbial production of short chain fatty acids derived from dietary fiber fermentation correlated with decreased colonocyte viability, possibly mediated by an increase in production of tumor pro-apoptotic cytokines by macrophages. Our work highlights the capacity of microfluidic *in vitro* models to study the role of microbial metabolism of dietary molecules on colorectal cancer colonocyte viability in the presence of macrophages.

Received 15th January 2025,
Accepted 8th September 2025

DOI: 10.1039/d5lc00052a

rsc.li/loc

Introduction

Dietary fiber consumption has been extensively associated with lower risk of colorectal cancer (CRC) in humans.[1] A causative link between consumption of dietary fiber in the form of inulin and decreased incidence of aberrant crypt foci and tumor formation in mice has also been reported.[2] Mechanistically, dietary fiber is metabolized by the colonic microbiota, which increases the abundance of fermentative bacteria and the production of short-chain fatty acids (SCFA) such as butyrate, propionate, and acetate.[3–5] The capacity of these metabolites to induce apoptosis in colonocyte *via* mechanisms such as histone deacetylase inhibition is well established.[6–11] For these reasons, prebiotic intervention with dietary fiber has been proposed as a preventive strategy against CRC.[12]

The colorectal tumor microenvironment contains multiple types of immune cells that significantly impact tumor development and progression.[13] Tumor-associated macrophages (TAMs) are abundant in carcinomas,[14,15] where they exhibit either tumor supportive activity by favoring cancer cell proliferation[16,17] and migration,[18–20] or tumor-suppressive activity by inducing tumor cell apoptosis *via* signals such as Tumor necrosis factor α (TNF-α)[21] and TRAIL.[22] The activity of TAM is influenced by host-derived molecules present in the tumor microenvironment such as cytokines, chemokines, non-coding RNA, and oncoproteins.[23,24]

In the colon, the microbiota and its metabolites have also been shown to modulate the activity of macrophages. Experiments in germ-free mice have shown that the microbiota regulates macrophage recruitment and replenishment after the onset of inflammation, possibly *via* induction of chemokine production in colonocytes.[25] Several pathogens associated with CRC, including *Fusobacterium nucleatum*, *Streptococcus gallolyticus*, and *Enterococcus faecalis*, promote a proinflammatory and immunosuppressive microenvironment by targeting macrophages.[26] In terms of bacterial metabolites, lipopolysaccharide is a potent inducer of

[a] *Department of Biomedical Engineering, Texas A&M University, USA. E-mail: arulj@tamu.edu*
[b] *Artie McFerrin Department of Chemical Engineering, Texas A&M University, USA*
[c] *Department of Medical Physiology, College of Medicine, Texas A&M University, USA*
[d] *Department of Electrical and Computer Engineering, Texas A&M University, USA*
† Equal contribution.

proinflammatory (M1-like) polarization in macrophages,[27] while the SCFA butyrate promotes anti-inflammatory (M2-like) polarization in macrophages while boosting their phagocytic activity.[28,29] Despite the high abundance of TAMs in tumors and the modulation of macrophage activity by microbiota, the effect of dietary fiber-induced changes in microbiota composition and function on TAM activity in CRC is not fully understood.

Intestinal and microfluidic models that facilitate the study of host-microbiota interactions, such as the gut-on-a-chip and HuMiX, have been successfully employed to gain insight into the effect of probiotics and prebiotics on epithelial physiology.[30–32] However, the interplay among dietary molecules, microbiota and immune cells in the context of CRC remains unexplored. Previously, we developed a microfluidic device to study the interaction between HCT116 CRC colonocyte spheroids and murine colonic microbiota.[33] Here, we expand the physiological relevance of this model by co-culturing a colonic microbial community with monocyte-derived macrophages with colonocytes in spheroids. We hypothesize that inulin fermentation by colonic microbiota impacts colonocyte viability in a macrophage-dependent manner. We use metabolomics, metagenomics, and protein and gene expression analysis to dissect the tripartite interaction between inulin, microbiota, and macrophages in our expanded CRC tumor microenvironment model. Our results contribute to our understanding of the effect of diet on host-microbiota interactions in the context of colorectal cancer and demonstrate the usefulness of physiologically relevant *in vitro* models to study these interactions.

Results

Inclusion of macrophages in an *in vitro* coculture model of CRC colonocyte-microbiota

To expand the physiological relevance of our previously developed colonocyte spheroid-microbiota coculture model,[33] we incorporated macrophages derived from the monocyte cell line THP-1 into spheroids. It is well-established that *in vitro* differentiation of THP-1 cells with PMA results in a macrophage-like phenotype, but the PMA concentration and treatment time widely vary among studies and significantly impact differentiation success.[34–36] Therefore, we first optimized PMA concentration and treatment time to maximize the development of macrophages and the expression of the macrophage surface marker cluster of differentiation 11b (CD11b). While THP-1 monocytes in culture are globular and remain in suspension, treatment of THP-1 cells with PMA resulted in cell attachment to the bottom of the culture plate with changes in both cell size and morphology (Fig. 1A). After PMA treatment for 24 h, the attached cells were circular in shape and displayed increased granularity under phase-contrast microscopy. As the treatment time increased beyond 48 h, cells became elongated at PMA concentrations greater than 50 ng mL^{-1}, while cells treated with lower concentrations remained globular and loosely attached. CD11b expression increased with treatment time and was maximum after 72 h of treatment with a PMA concentration of 50 ng mL^{-1}, as assessed by flow cytometry. Minimal differences in cell morphology were observed with higher PMA concentrations for the same duration of PMA stimulation (Fig. 1A). Under these conditions, the mean fluorescence intensity in PMA-treated cells (indicative of Cd11b levels) increased 75% compared to untreated cells (Fig. 1B and C). In addition, gene expression analysis revealed a significant upregulation in the transcription of genes related to monocyte differentiation and macrophage activity, including CD40, CD44, CD80, TNF-α, CD206, and CD163 (Fig. S1). Therefore, treatment with a PMA concentration of 50 ng mL^{-1} for 72 h was selected to induce THP-1 differentiation in all subsequent microfluidic device experiments.

After optimizing THP-1 differentiation conditions, we cocultured HCT116 colonocytes and THP-1 cells in our previously developed model of colonocyte-microbiota interactions in colorectal cancer.[33] In this model, colorectal cancer spheroids and colonic microbiota are cultured in separate, continuously perfused compartments and exchange secreted metabolites through a porous membrane (Fig. 2A–C). To include macrophages in this model, a 1 : 1 suspension of THP-1 monocytes and HCT116 colonocytes in Matrigel was injected in the mammalian cell culture chamber on day 0 and perfused with media containing the optimized PMA concentration for 3 days to foster monocyte polarization during colonocyte spheroid formation before coculture with microbiota and/or treatment with inulin (Fig. 2D). Treatment with PMA during co-culture with HCT116 cells resulted in a significant increase in the expression of CD11b in THP-1 cells, with 60% of cells becoming positive and a 2.5-fold increase in MFI compared to untreated THP-1 monocytes in flask cultures (Fig. 2E and F). To better understand the contribution of different factors to CD11b overexpression, we exposed Matrigel-embedded THP-1 cells to HCT116 in co-culture, PMA treatment, or combinatorial treatment, using transwell inserts (Fig. S2A). Gene expression analysis revealed that both HCT116 alone or PMA alone increased the transcription of CD11b in THP-1 cells, while combinatorial treatment resulted in the highest expression levels (Fig. S2B). These results confirmed the differentiation of THP-1 cells into a macrophage-like phenotype in the microfluidic coculture model.

Inulin induces changes in microbiota abundance and function

To validate the use of our model to study the impact of dietary fiber on microbiota, we characterized the effect of inulin treatment on SCFA production and alterations in microbiota composition. The levels of three SCFAs (acetate, propionate, and butyrate) produced by anaerobic microbiota co-cultured with HCT116 cells after inulin treatment were analyzed using GC-MS. Treatment with inulin for 12 h resulted in a 95% (from 234 μM to 12 μM) decrease in acetate and a less pronounced decrease of 44% (from 12 μM to 7 μM) in butyrate levels, relative to the untreated controls. On the other hand, a 25% increase (from 50 μM to 63 μM) in

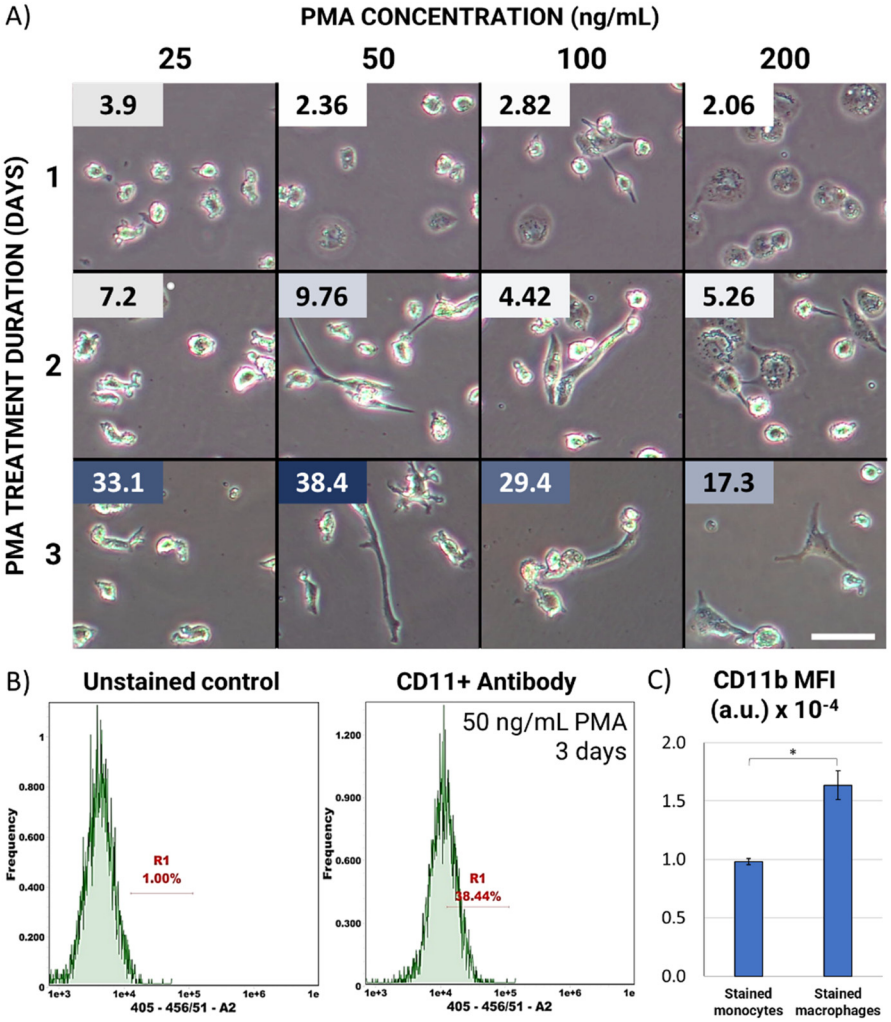

Fig. 1 Optimization of PMA treatment for THP-1 monocyte differentiation. A) Morphology of THP-1 cells after treatment with PMA in well plate. Boxed number indicates percentage of CD11b+ cells. Scale bar = 100 μm. B) Representative histograms of PMA-treated THP-1 cells stained with a fluorescently labelled CD11b antibody, and unstained control to account for background fluorescence. C) Mean fluorescent intensity (MFI) of stained THP-1 "monocytes" (untreated) and "macrophages" (PMA-treated, 50 ng mL^{-1} for 3 days). * p-value < 0.05, $n = 3$. Error bars represent SEM.

propionate levels was observed (Fig. 3A), indicating differential effect of inulin exposure on the production of SCFAs by the microbial community. Inulin treatment also induced bacterial proliferation, as noticed by a 21% increase in the optical density of the culture at 600 nm (Fig. 3B).

Metagenomic (16S rRNA) analysis of the microbiota community after inulin treatment revealed minimal taxonomic changes in the composition. Regardless of inulin treatment, the microbiota cultured on chip was dominated by members of the *Bacteroides* genus (70%), and 24 other genera commonly associated with gastrointestinal tract microbiota, such as *Blautia*, *Ruminococcus*, and *Akkermansia*, that were present at a relative abundance higher than 1% (Fig. 3C). The β-diversity analysis shows that while inulin treatment resulted in a significant change in overall microbiota composition, there was an overlap between ellipses that define a 95% confidence interval around the centroid of each treatment (Fig. 3D). This result is consistent with the small but significant change in the abundance of members of the community upon treatment with inulin, including *Akkermansia* (0.45-fold), *Dysgonomonas* (0.88-fold), *Oscillospira* (0.87-fold), *Anaerostipes* (1.96-fold), and *Lactobacillus* (1.62-fold) (Fig. 3E), as well as a 1.2-fold increase in the relative abundance of 7 genera (*Pseudobutyrivibrio, Anaerotruncus, Anaerobranca, Erysipelothrix, Turicibacter, Lachnospira, Peptoniphilus*) that did not reach statistical significance. The largest effect of inulin on microbiota composition was a 4% increase in the abundance of the genus *Bacteroidetes*, while the largest change in relative composition was a 1.96-fold increase in the abundance of the genus *Anaerostipes*.

Inulin enhances macrophage-mediated decrease in colonocyte viability in a microbiota-dependent manner

To evaluate the impact of inulin on macrophage-microbiota-colonocyte interactions, we cocultured HCT116 colonocytes with

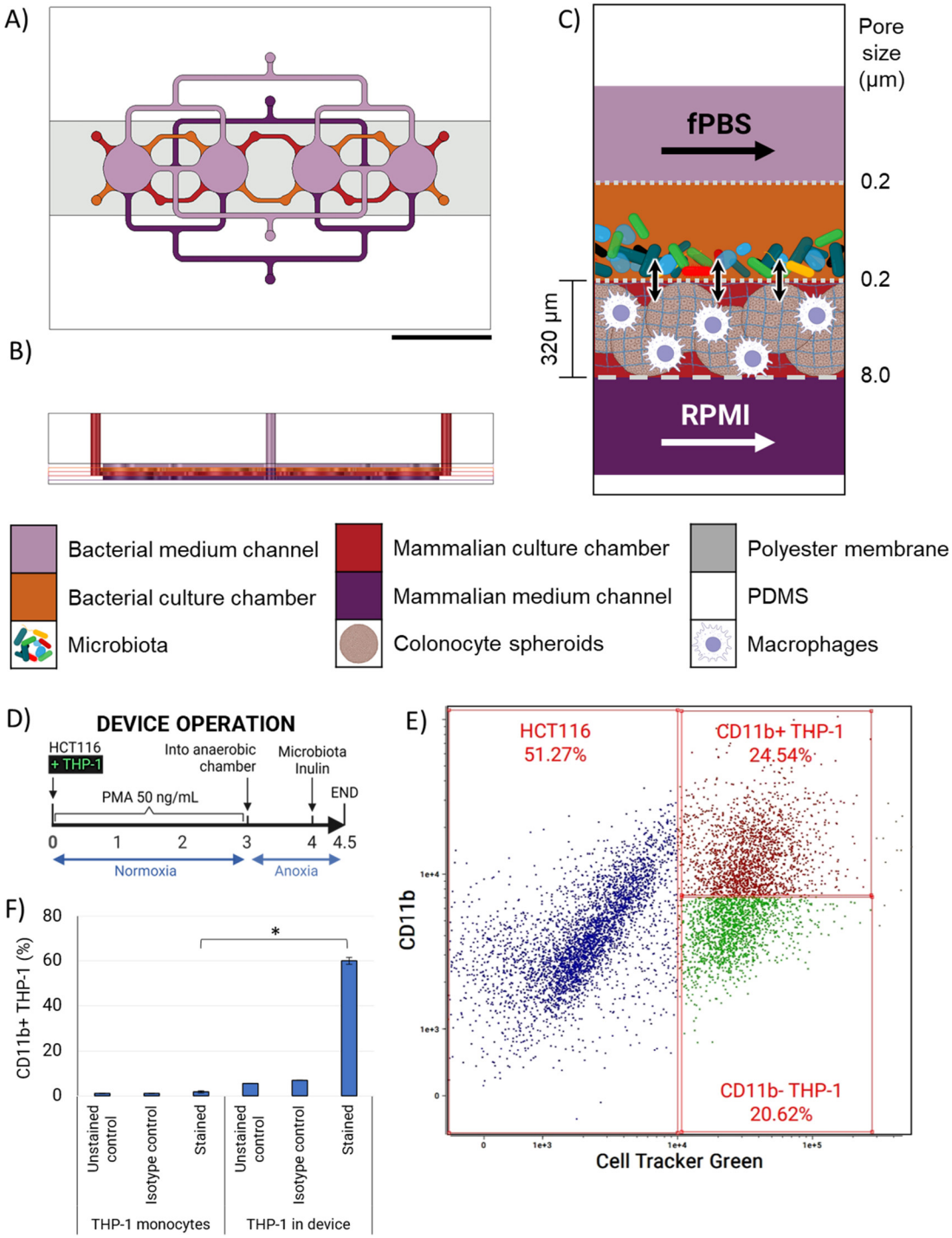

Fig. 2 Microfluidic device design and operation. A) Top and B) cross-sectional views highlighting media channels and culture chambers. Scale bar = 1 cm. C) Schematic representation of device cocultures. Confined bacterial, colonocyte and macrophage populations interact *via* small molecules during perfusion of fecal PBS (fPBS) through the top channel and growth media (RPMI) through the bottom channel. D) Experimental schedule of device coculture. E) Dot-plot of HCT116 – THP-1 cells after device coculture. THP-1 cells were loaded with CellTracker green dye prior to coculture. The CD11b positivity threshold was defined based on unstained control. F) Percentage of CD11b+ THP-1 monocytes (control) and THP-1 cells after treatment with PMA during device coculture. * p-value < 0.05, $n = 3$. Error bars represent SEM.

THP-1 macrophages and microbiota for 12 hours (Fig. 4A). HCT116 spheroids without THP-1 macrophages, HCT116 spheroids and microbiota without THP-1 macrophages, and HCT-116, THP-1, and microbiota without inulin were used as controls to assess the impact of each component on HCT116 cell viability. After device coculture and treatment, cells were extracted from the device and disaggregated into a single cell suspension. The viability of each cell type was assessed

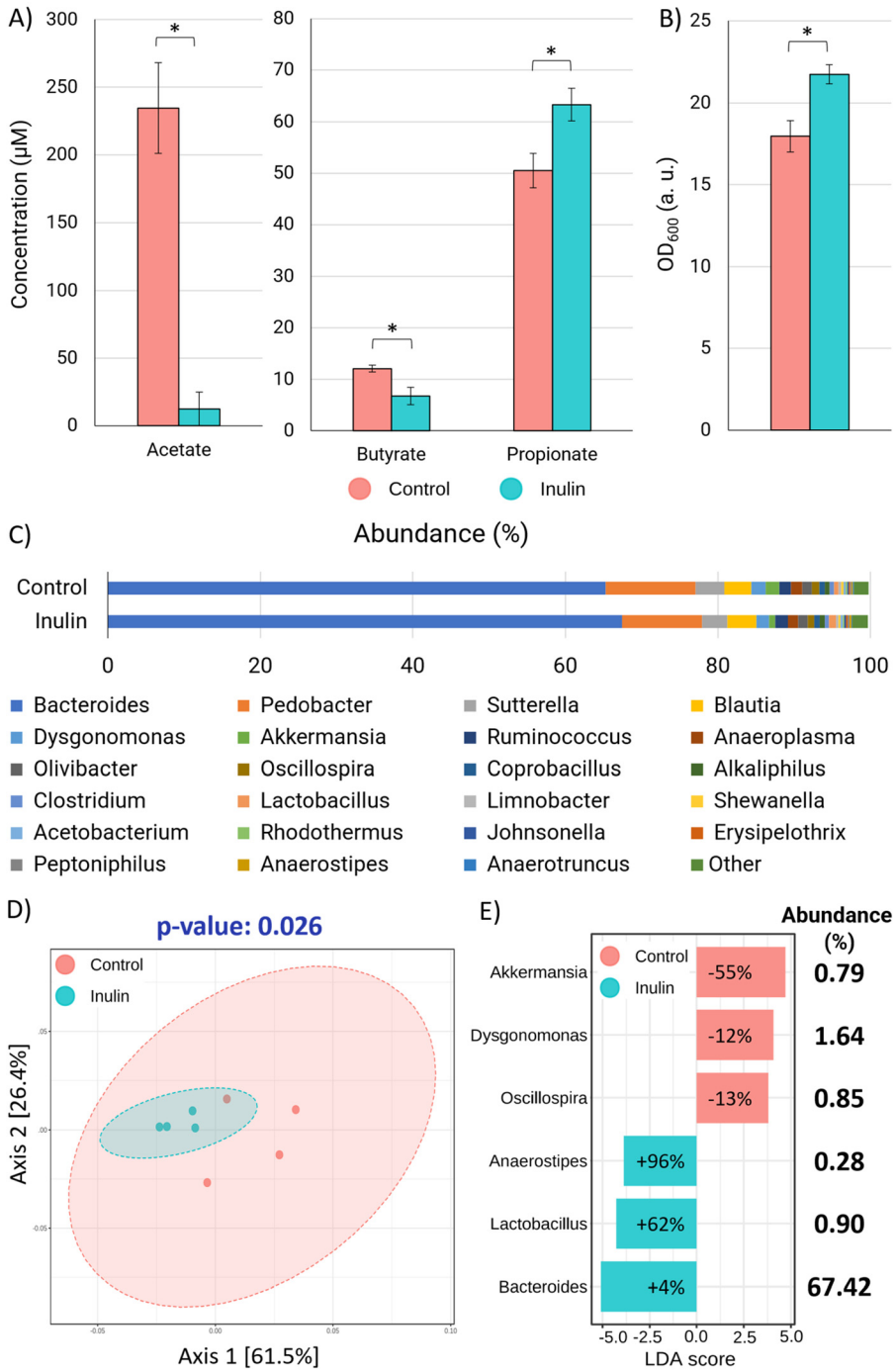

Fig. 3 Effect of inulin on microbiota function, abundance, and composition. A) SCFA concentration in the bacterial culture chamber upon treatment with fPBS supplemented with 2.5% (w/v) inulin. B) Optical density of microbiota extracted from the device after inulin treatment. * p-value < 0.05, $n = 3$. C) Microbiota composition at the genus level, D) β-diversity analysis, and E) LEfSe comparison of microbiota after treatment with inulin (2.5 % w/v in fPBS) or control (fPBS) on chip. Percentages in the bars in E) correspond to relative change in the abundance of a genera normalized to abundance in control, and abundance (%) corresponds to the composition in the inulin-treated microbiota.

employing a combination of CellTracker Green dye for labelling THP-1 cells and PI staining for labelling dead cells (Fig. 4B). Inulin treatment of microbiota in coculture with HCT116 colonocytes and THP-1 macrophages resulted in a decrease of 17% in colonocyte viability relative to control treatments without macrophages, microbiota, or inulin (Fig. 4C). In contrast, THP-1 viability remained relatively unchanged, regardless of the presence of microbiota or treatment with inulin (Fig. 4D). The reduction in colonocyte viability correlated with a 4-fold increase in TNF-α transcription with respect to cocultures without either microbiota or inulin (Fig. 4E), suggesting an effect of inulin metabolism by the microbiota on

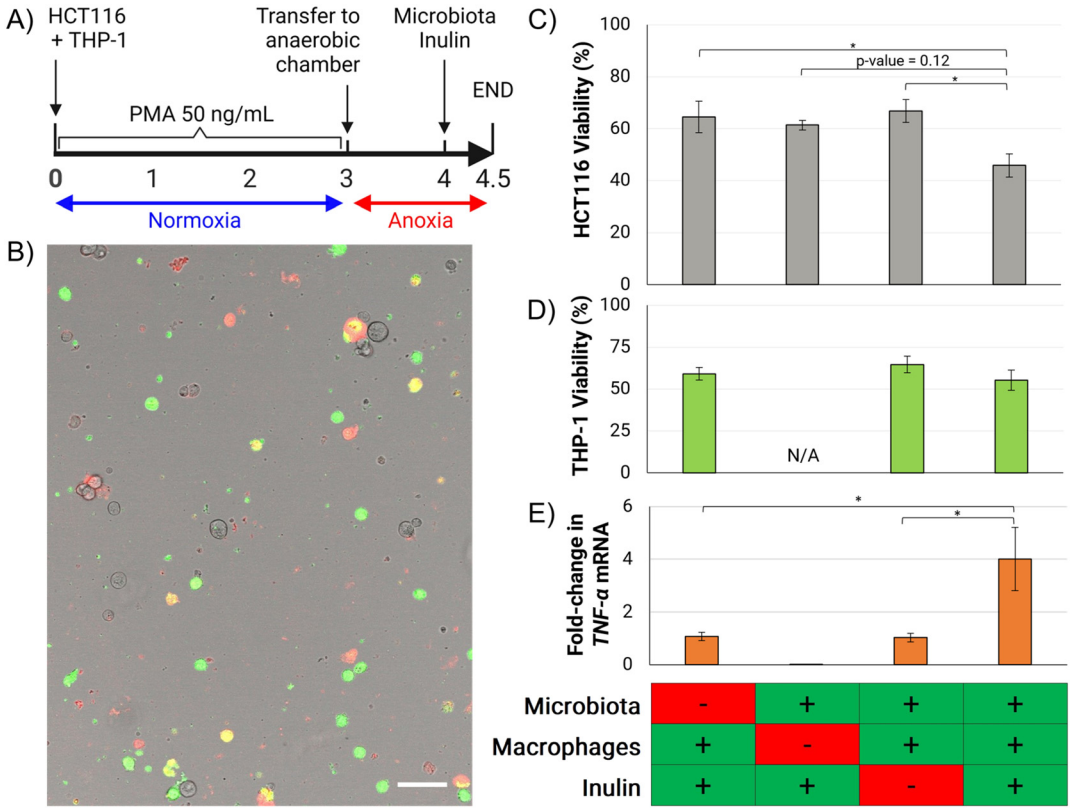

Fig. 4 Effect of macrophages, inulin, and microbiota on colonocyte viability. A) Experimental schedule. B) Representative image of multicolor strategy to distinguish viability by cell type after extraction of cells from microfluidic device. Unstained: viable HCT116 cells. Red: dead HCT116 cells. Green: viable THP-1 cells. Yellow: dead THP-1 cells (green + red). Scale bar = 50 μm. C) HCT116 and D) THP-1 viability upon combinatorial treatment with microbiota and inulin. E) Associated fold-change in TNF-α transcription in device co-cultures. * p-value < 0.05, $n = 3$. Error bars represent SEM.

pro-inflammatory cytokine production and macrophage-colonocyte interaction.

Inulin-derived SCFAs increase the concentration of pro-inflammatory cytokines during THP-1- HCT116 co-culture

To gain deeper understanding of the mechanisms through which microbial fermentation of inulin might increase macrophage toxicity against cancer cells, HCT116 and THP-1 cells transwell co-cultures were treated with prepared SCFA mixtures matching the SCFA concentrations measured from inulin-treated devices' co-cultures ("inulin-derived SCFA"), control devices without inulin ("inulin-negative SCFA"), and monoculture controls, following the same experimental schedule as device co-cultures (Fig. 5A). Quantification of culture supernatants for pro-inflammatory cytokines revealed a significant upregulation of IL-1β, IFN-γ, TNF-α, MCP-1, IL-8, IL-12p70 and IL23 after treatment of co-cultures with inulin-derived SCFA mixture, compared to control (Fig. 5B). In addition, the cytokine IL-33, which was undetectable in control co-cultures, also followed this trend; however, since the levels were below the limit of detection in control cultures, it was not possible to assign statistical significance. Individual treatment of each cell type with the SCFA mixtures suggested HCT116 as the cell type likely responsible for the increased production of MCP-1, IL-23, TNF-α and IL-33, while THP-1 was identified as the likely producer of IL-1β and IL12p70 (Fig. 5B). Interestingly, co-culture of THP-1 macrophages with HCT116 cells significantly reduced the concentration of the aforementioned cytokines, and treatment with inulin-derived SCFA mixture partially recovered pro-inflammatory cytokine levels.

Discussion

Dietary fiber intake significantly correlates with decreased incidence of CRC in prospective human cohort studies.[1,37] Administration of inulin to murine CRC models has been shown to result in altered microbial abundance, changes in microbiota composition, and modulation of SCFA production.[2,38] In our model, inulin treatment significantly increased microbial proliferation and abundance (Fig. 3B), which agrees with the reported increase in cecal weight in mice and rats that has been partly attributed to increased bacterial abundance.[39,40] Inulin treatment also statistically altered the overall composition of the microbiota, although the impact on the abundance of most genera was not significant (Fig. 3C and D). Members from the genus *Bacteroides*, an abundant member of human and murine intestinal microbiota

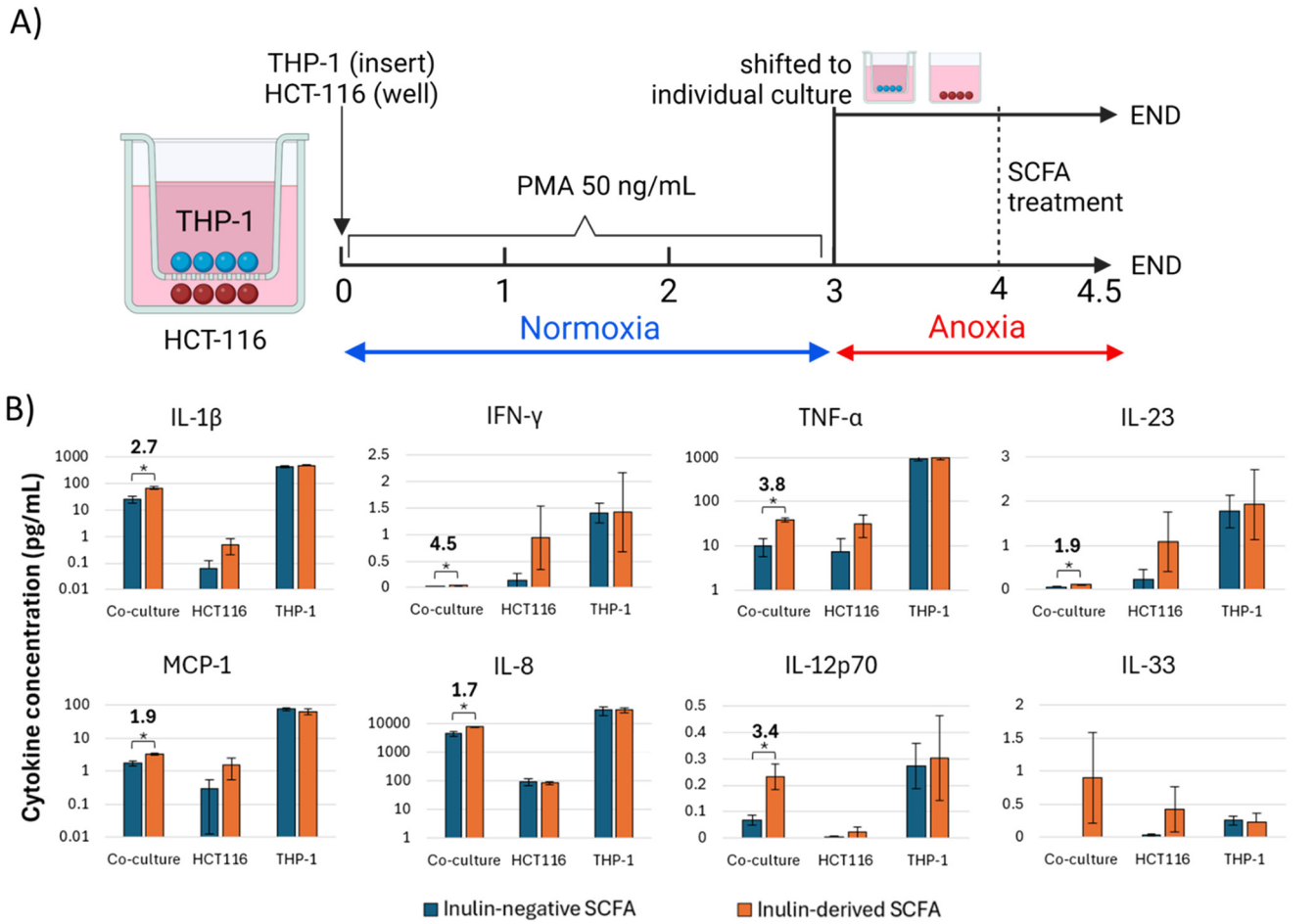

Fig. 5 Effect of inulin-derived SCFA mixture on pro-inflammatory cytokine levels. A) Experimental design of co-culture and mono-culture treatment with SCFA mixtures. B) Quantified pro-inflammatory cytokine concentrations. Bold number above bars indicate fold change in cytokine concentration, normalized to "inulin-negative SCFA". * p-value < 0.05, $n = 3$. Error bars represent SEM.

that outcompetes other inulin fermenters such as Bifidobacteria *in vitro,*[41] were detected in the microbiota cultured in our model and increased in abundance with inulin treatment. Therefore, the small impact of inulin on the overall microbiota composition could be a consequence of interspecies competition dominated by *Bacteroidetes* (Fig. 3E). The abundance of the genera *Lactobacillus* and *Anaerostipes*, reported to increase in individuals upon ingestion of inulin,[42–45] also significantly increased in our model.

Inulin treatment resulted in a significant increase in propionate (Fig. 3A), which is the most consistently reported effect of inulin administration in murine models.[46–51] The increase in propionate concentration also agrees with the high abundance of *Bacteroides* in the community, as members of this genus ferment inulin into propionate.[52,53] The effect of inulin administration on the levels of acetate in the colon *in vivo* have been inconsistent, with at least two studies showing either no effect or a decrease in abundance.[46,48] In our model, inulin treatment resulted in a significant decrease in extracellular acetate, which might have been caused by the conversion of acetate into acetyl-CoA for fatty acid biosynthesis and TCA cycle intermediates under low oxygen conditions to support proliferation.[54] While inulin consumption is frequently associated with increased butyrate levels in mice and rats,[47–49,51] a decrease in butyrate was observed in our model. Crucially, inulin and fructose fermenters are known to produce acetate that is then employed by other species to produce butyrate;[55] therefore, the lack of an increase in butyrate could simply be a consequence of the short treatment time (12 hours) compared to weeks of inulin feeding in *in vivo* experiments.[46–51] It is also important to highlight that the response of gastrointestinal microbiota to dietary fiber interventions *in vivo* is heavily dependent on initial microbiota composition, which has resulted in significant inter-subject and inter-study variability[56–59] and may explain the differences between some of our results and other studies. Overall, our model recapitulated the increase in microbiota abundance and changes in SCFA production induced by inulin *in vivo*, which supports its use to study the effect of this dietary fiber on colonic microbiota *in vitro*.

Based on the immunomodulatory activity of the microbiota in the colon and the pivotal role of macrophages in CRC, we hypothesized that the changes in microbiota induced by inulin impact macrophage–colonocyte interaction in our coculture

model. Our results show a macrophage-dependent decrease in colonocyte viability upon coculture with microbiota treated with inulin (Fig. 4C). This correlated with an increase in the transcription and secretion of TNF-α in the co-cultures (Fig. 4E and 5B), a proinflammatory cytokine that triggers apoptosis and necrosis in tumor-derived cell lines,[21] including CRC cell lines.[60,61] The increase in TNF-α production correlated with a decrease in acetate and an increase in propionate with inulin-treated device co-cultures (Fig. 3A), which agrees with the reported strong inhibition of TNF-α production by acetate.[62] Treatment of THP-1 and HCT116 colonocyte transwell co-cultures with a mixture of SCFA matching the concentrations from inulin-exposed device cocultures confirmed an increase in the abundance of proinflammatory cytokines (Fig. 5B) that have been reported to promote macrophage recruitment and activation (MCP-1, IL-8),[63,64] phagocytic activity (IL-23),[65,66] and tumor cell apoptotic induction by macrophages (IL-12p70, IFN-γ).[67–69] While these observations might explain the macrophage-dependent decrease in colonocyte viability upon treatment with inulin, the mechanisms associated with the possible role of these cytokines in this context require further study.

Importantly, cytokines such as IL-23 and IL-8 can also induce cancer cell proliferation[70,71] in a matter that might be dependent on the action of multiple immune cells in the tumor microenvironment;[13] therefore, increased model complexity by incorporating additional immune cell types such as T- cells will likely improve the physiological relevance and elucidation of underlying mechanisms. Inulin-induced changes in the abundance of other microbial metabolites that affect pro-inflammatory cytokine production in macrophages, such as lipopolysaccharide and indole derivatives,[72] may also explain the observed effect of inulin on colonocyte viability, and require further characterization.

A strong association between dietary fiber consumption and lower CRC incidence has been reported by metanalyses of prospective cohort studies.[1,37] The preventive activity of dietary fiber against colorectal cancer has been attributed to the increased production of total SCFA by microbiota and its direct proapoptotic effect on colonocytes.[73,74] Importantly, a large number of dietary intervention studies in humans have found little to no effect of inulin ingestion on fecal SCFA concentration.[75–80] Our results suggest that dietary fiber may reduce cancer colonocyte viability *via* proinflammatory cytokine production in macrophage and cancer cell co-cultures, even in the context of a decreased total abundance of SCFA. The microbiota-mediated immunomodulatory activity by inulin proposed here is conceptually similar to the improved Natural Killer cell cytotoxicity in a rat model of CRC upon inulin administration,[81] as well as the reduction in xenograft tumor growth in mice upon inulin administration *via* microbiota-dependent T-cell activation.[82] Since both diet and immune cell activity are key factors in CRC, the mechanisms underlying the potential immunomodulatory effect of dietary fiber on the immune component of the tumor microenvironment require further study.

The role of macrophages in CRC is controversial.[83,84] While *in vitro* studies have shown that macrophages induce CRC colonocyte proliferation and migration,[16–20] epidemiological studies show that high macrophage infiltration in CRC tumors is often associated with better prognosis.[85] Importantly, *in vitro* studies have failed to consider the hypoxic, ECM-rich, three-dimensional microenvironment of tumor tissue,[13] as well as the impact of the microbiota and its products on macrophage activity. Our results using a physiologically-relevant microenvironment that contains both microbiota and dietary molecules show a macrophage-dependent decrease in colonocyte viability *in vitro*, more consistent with epidemiological data. We also identified an increase in the abundance of inflammatory cytokines upon inulin-derived SCFA treatment in a complex macrophage-cancer cell co-culture, while treatment of monocultures failed to capture these effects. These observations support the potential of complex *in vitro* systems and microfluidic technology to study complex host-microbiota interactions *in vitro* in a manner that is more relevant than conventional cell culture experiments.[86]

Future endeavors on model development and biological characterization are poised to increase the impact of our findings. Current co-cultures with microbiota last for 12 hours, which is sufficient to observe significant changes at the transcription and translation levels. However, extended fermentation times of up to 24 hours might be required to ensure complete inulin consumption and more significant changes in microbiota composition.[87,88] While the changes in microbiota composition upon inulin treatment we observed are consistent with reported effects of inulin *in vivo*, a more extended coculture time might be required to observe more pronounced changes in composition which would better recapitulate the shifts in composition observed *in vivo.* The mechanisms of inulin-microbiota-macrophage interaction proposed here are based on correlation among variables and, therefore, require further investigation to demonstrate causality. This could be accomplished by employing selective inhibitors (*e.g.*, against TNF activity),[89] using synthetic or controlled microbial communities,[59] and macrophages with diminished TNF-α production capacity.[90] Further characterization of the microbiota *via* metabolomics, as well as macrophages *via* RNA sequencing and expanded immunotyping, would be useful to identify correlations between microbial metabolism, macrophage activation, and colonocyte viability. The use of more relevant sources of macrophages, such as bone-marrow derived monocytes, would also increase the biological relevance of future studies.[91] Finally, a diverse group of dietary fibers may increase our understanding of the dynamics of dietary fiber fermentation and changes in microbiota and macrophage activity.

Methods

Mammalian cell culture and reagents

The human colorectal cancer cell line HCT116 (CCL-247) was obtained from ATCC and cultured in RPMI 1640 medium

(Corning) supplemented with 10% FBS (Atlanta Biologicals), GlutaMAX, HEPES, and NEAA (Gibco). The human monocyte cell line THP-1 was obtained from ATCC and cultured in RPMI 1640 medium (Corning) supplemented with 10% FBS (Atlanta Biologicals), 1% GlutaMAX, 1% HEPES, 1% NEAA (Gibco), and 2-mercaptoethanol (Sigma-Aldrich) to a final concentration of 0.05 mM. THP-1 cultures were maintained at a density between 2×10^5 and 9×10^5 cells per mL. For device coculture experiments, THP-1 cells were labelled with 2 μM CellTracker Green CMFDA (ThermoFischer Scientific) in serum-free media for 45 minutes.

Optimization of THP-1 differentiation

THP-1 monocytes were differentiated to macrophages with phorbol 12-myristate 13-acetate (PMA, Sigma-Aldrich). THP-1 differentiation was optimized using $\sim 5 \times 10^5$ cells per mL in a 1 mL culture tube and treated with PMA to a final concentration of 25, 50, 100 or 200 ng mL^{-1}. Cells were incubated at 37 °C for 1, 2, or 3 days. To detach PMA-treated THP-1 cells from culture tubes for flow cytometry analysis, the PMA-containing media was replaced with PBS with 10 mM EDTA, incubated on ice for 15 minutes, and detached by repeated pipetting.

Microfluidic device construction and operation

Device construction and operation was performed as previously described.[33] The device consists of four PDMS layers separated by three porous polyester membranes (Fig. 2A–C). Thin patterned PDMS layers were obtained by pouring uncured PDMS mix (Sylgard 184®) on a 3D-printed patterned mold (Stratasys, Inc.) with a total height of 500 μm and a pattern height of 160 μm, and then the PDMS was cured for 1 hour at 70 °C. Biopsy punches were used to create culture chambers (D = 5 mm, final chamber volume of ~10 μL) and open access to the perfusion channels and culture chambers (D = 1 mm). The device was assembled layer-by-layer using a thin layer of uncured PDMS as glue, and a polyester membrane was sandwiched between each pair of layers. The device was connected to media reservoirs by flexible 23-Gauge Tygon® medical tubing (Saint Gobain) using 20-Gauge stainless steel connectors detached from dispensing needles (Jensen Tools). To minimize the formation of bubbles during operation, the assembled device was placed underwater and vacuumed to a final pressure of 3×10^{-2} mbar for 24 hours; then, the device was autoclaved (121 C, 16 PSIG, 45 minutes) and kept covered in sterile water during operation. This protocol sterilized the device and prevented bubble formation. The device was held underwater for the duration of the experiment and only brought out of water for cell injection.

For colonocyte injection, the mammalian culture chambers in the device were seeded with 50% v/v Matrigel diluted in RPMI medium containing either $\sim 4 \times 10^6$ HCT116 cells per mL or $\sim 2 \times 10^6$ HCT116 and $\sim 2 \times 10^6$ labelled THP-1 cells per mL. After cell seeding, devices were perfused with antibiotic-free RPMI through the mammalian medium channel, while PBS supplemented with 50 ng mL^{-1} of PMA was perfused through the bacterial chamber. On day 4 of culture, the bacterial chamber media was replaced with PMA-free PBS, and devices were transferred and operated in an anaerobic chamber for 24 hours. On day 5, murine fecal microbiota was obtained from freshly-voided fecal pellets obtained from 8 to 12 weeks-old wild-type C57BL/6 female mice fed a standard chow diet and processed as previously described to isolate microbiota and prepare fecal PBS (fPBS).[33] The fecal slurry containing microbiota was introduced into the bacterial chamber, and the PBS in the bacterial medium reservoir was replaced with sterile-filtered fPBS or fPBS supplemented with inulin at a concentration of 2.5% (w/v) (Spectrum Chemical). Cocultures proceeded for 12 hours.

For sample collection, the microbiota in the bacterial culture chamber was collected by pipetting, to a final volume of ~10 μL per chamber. Bacteria were pelleted by centrifugation at 10 000 g for 10 minutes. The supernatant was used for SCFA analysis by GC-MS while the bacterial pellet was resuspended in 500 μL of PBS, the OD_{600} noted, and centrifuged (10 000 g, 10 minutes) to obtain a bacterial cell pellet. All pellets were stored at −80 °C until further processing. Next, the mammalian hydrogels were recovered by carefully disassembling the device with a scalpel. For flow cytometry and viability analysis, the mammalian hydrogels were placed on ice in PBS with 10 mM EDTA for 15 minutes and disaggregated by repeated pipetting to obtain single cell suspensions. For gene expression analysis, hydrogels were directly lysed on cell lysis buffer (RLT buffer, QIAGEN) and stored at −80 °C until further processing.

Immunostaining and flow cytometry

For immunostaining, Fc blocking was performed using human IgG (Sigma-Aldrich) at a concentration of 4 μg/10^6 cells for 15 minutes at room temperature. Cells were stained with Human CD11b/Integrin alpha M Alexa Fluor® 405-conjugated Antibody (R&D Systems) at a concentration of 1 μg/10^6 cells according to manufacturer's protocols, using normal mouse IgG2b Alexa Fluor 405 (Santa Cruz Biotechnology) as isotype control. Flow cytometry was performed using a CellStream benchtop flow cytometer (Millipore Sigma). Single color controls were used to create a compensation matrix for signal bleed between fluorophores. Single cells were acquired using a 0.6–1 Aspect Ratio as the criterion. Dead cells were excluded with Propidium Iodide (PI) staining (1.5 μM for 5 minutes). Mean fluorescence intensity per cell and cell counts were obtained directly from CellStream™ Software (Millipore Sigma).

Mammalian cell viability evaluation

Single cell suspensions were stained with 1.5 μM PI and incubated for 15 minutes in the dark at room temperature. Viability was evaluated using a Leica TCS SP5 confocal

microscope. At least 100 cells were counted per sample, and 4 hydrogels were processed per treatment.

SCFA analysis

SCFA quantification was carried out by the Integrated Metabolomics Analysis Core at Texas A&M University. Metabolites were extracted from samples using ethyl acetate and the levels of 6 SCFAs (acetic, butyric, isobutyric, isovaleric, propionic, and valeric acid) were quantified using GC-MS. Isotopically labelled n-butyrate was used as the internal control and was spiked into all samples prior to extraction. Samples were diluted 10-fold in PBS before extraction. SCFAs were detected and quantified on a gas chromatography triple quadrupole mass spectrometer (TSQ EVO 8000, Thermo Scientific, Waltham, MA). Chromatographic separation was achieved on a ZB WAX Plus, 30 m × 0.25 mm × 0.25 μm column (Phenomenex). The MS data and retention times were acquired in full scan mode from m/z 40–500 for the individual target compounds. The injector, MS transfer line and ion source were maintained at 230 °C, 240 °C and 240 °C respectively. The flow rate of helium carrier gas was kept at 1 mL min^{-1}. Samples were maintained at room temperature on an autosampler before injection. 1 μl of the extracted sample was injected with a split ratio of 20 : 1. The ionization was carried out in the electron impact (EI) mode at 70 eV. Sample acquisition and analysis was performed with TraceFinder 3.3 (Thermo Scientific).

Microbiota composition analysis

DNA from bacterial communities was extracted by using the DNeasy PowerSoil Kit (QIAGEN) according to manufacturer's instructions, and the v4 region of the 16S rRNA gene was sequenced using the MiSeq Illumina Platform (FERA Diagnostics and Biologicals). Bioinformatic analysis was performed using Microbiome Analyst (**https://www.microbiomeanalyst.ca**) at the genus level. Features with singlets were removed prior to analysis. Features with single readings were removed before analysis. For comparative analysis, only features with a read count higher than 4 in 50% of samples were included, and 10% of features with the lowest coefficient of variation were removed to ameliorate data sparsity and improve statistical power.[92] Data was scaled using cumulative sum scaling. The Bradis-Curtis index distance metric was used with PERMANOVA as the statistical method. LEfSe analysis was performed using LDA > 2.0 as the significance filter and $p < 0.05$ was used for statistical significance.

Gene expression analysis

RNA was extracted from mammalian cells using the RNeasy Mini Kit (QIAGEN) following the manufacturer's instructions. Genomic DNA in the extracted RNA was eliminated by digesting with DNAse (QIAGEN). cDNA synthesis was performed using qScript™ cDNA SuperMix (QuantaBio) using 100 ng of RNA sample in a 10 μL reaction. Quantitative PCR was carried out in a Lightcycler® 96 (Roche) using FastStart Universal SYBR Green Master (Roche). Primers were designed using Primer Blast (NCBI), and amplicon size and specificity were confirmed by melting peak analysis and agarose gel electrophoresis of the reaction products. Each reaction mix contained 1/40th of the cDNA pool obtained per sample and a total primer concentration of 400 nM. The PCR regime consisted of preincubation for 10 minutes at 95 °C and 45 amplification cycles (95 °C × 15 s, 65 °C × 30 s, 72 °C × 45 s). Data were processed using the $2^{-\Delta\Delta Ct}$ method. Multiple genes were evaluated as endogenous qPCR controls, including 18 s, YWHAZ, PMM1, UBC, IPO8, and VPS29; from these genes, PMM1 showed the most stable expression level and was employed as endogenous control. Sequences for all used primers are provided in Table 1.

Statistical analysis

For testing statistical significance, unpaired Student's t-tests were performed on sets of data with two experimental conditions. One-way ANOVAs were used for comparisons among multiple experimental conditions and during RTqPCR data analysis. For RTqPCR data analysis, significance in gene expression changes was determined by comparing ΔCt values across treatments, as gene expression data is log-normally distributed.[93] The assumption of equality of variances among data sets was confirmed by using the Levene's test, and normality was validated using the Shapiro–Wilk test. All experiments were performed at least in duplicate, and coculture experiments were performed in triplicate.

Table 1 Primer sequences for gene expression analysis

Gene	Forward primer	Reverse primer
PMM1	GTGTTCCCCATGCTCCACCT	ATAGGCACCTTCCCCACCGT
TNF-α	CTCTTCTGCCTGCTGCQCTTTG	ATGGGCTACAGGCTTGTCACTC
CD80	CTCTTGGTGCTGGCTGGTCTTT	GCCAGTAGATGCGAGTTTGTGC
CD44	CCAGAAGGAACAGTGGTTTGGC	ACTGTCCTCTGGGCTTGGTGTT
CD40	CCTGTTTGCCATCCTCTTGGTG	AGCAGTGTTGGAGCCAGGAAGA
CD11b	GGAACGCCATTGTCTGCTTTCG	ATGCTGAGGTCATCCTGGCAGA
CD86	CTGCTCATCTATACACGGTTACC	GGAACGTCGTACAGTTCTGTG
CD68	CTTCTCTCATTCCCCTATGGACA	GAAGGACACATTGTACTCCACC
CD206	GGGTTGCTATCACTCTCTATGC	TTTCTTGTCTGTTGCCGTAGTT
CD163	TTTGTCAACTTGAGTCCCTTCAC	TCCCGCTACACTTGTTTTCAC

Effect of SCFA on cytokine production during transwell co-cultures

To study the effect of SCFA on the THP-1 and HCT116 co-culture, 50 μL of Matrigel containing ~2.5 × 10^6 cell per mL of HCT 116 and ~2.5 × 10^6 cell per mL of THP-1 were seeded in a 24 well transwell plate in the well and the insert, respectively. RPMI media containing 50 ng mL^{-1} PMA was added to the well (600 μL) and insert (300 μL) and kept in co-culture. After 72 hours, the plate was transferred in an anaerobic chamber and the media replaced with fresh RPMI media with PMA. The THP-1 containing transwells were either shifted to a different well to study the individual culture or kept in the co-culture for 24 hours. Cells were then treated for 12 hours with RPMI medium containing sodium acetate, sodium butyrate, and sodium propionate at concentrations previously measured in device co-cultures (μM): 234.6, 12.1, 50.5 ("inulin-negative SCFA"); 12.55, 6.7, 63.3 ("inulin-derived SCFA"), respectively. Cell supernatants were collected and stored at −80 °C for cytokine analysis.

Multiplex cytokine analysis

Stored cell supernatants were centrifuged at 300 × *g* for 4 min to remove cell debris and the supernatant was then analyzed for a panel of 13 inflammatory cytokines using the LegendPlex Human Inflammation Panel (13-Plex) (BioLegend), according to manufacturer's instructions. Samples were analyzed *via* flow cytometry using a Cytek Aurora Spectral Flow Cytometer (Cytek Biosciences).

Author contributions

D. P., M. M., and A. J. designed the research. D. P. and M. M. performed the experiments. D. P., M. M., S. C., A. H. and A. J. analyzed the data. D. P., M. M., and A. J. wrote the article with input from A. H and S. C. All authors reviewed, discussed, and edited the manuscript.

Conflicts of interest

The authors declare that they do not have any competing interests.

Data availability

Supplementary information is available. See DOI: **https://doi.org/10.1039/D5LC00052A**.

The data supporting this article have been included as part of the SI.

Acknowledgements

This work was partially supported by funds from the Ray B. Nesbitt Chair endowment to A. J. The authors acknowledge use of facilities at the Integrated Metabolomics Analysis Core (IMAC) at Texas A&M University.

References

1 S. K. Veettil, T. Y. Wong, Y. S. Loo, M. C. Playdon, N. M. Lai and E. L. Giovannucci, *et al.*, Role of Diet in Colorectal Cancer Incidence: Umbrella Review of Meta-analyses of Prospective Observational Studies, *JAMA Netw Open*, 2021, **4**(2), e2037341, DOI: **10.1001/jamanetworkopen.2020.37341**.

2 B. L. Pool-Zobel, Inulin-type fructans and reduction in colon cancer risk: review of experimental and human data, *J. Geophys. Res.:Oceans*, 2005, **93**(Suppl 1), S73–S90, DOI: **10.1079/bjn20041349**.

3 D. So, K. Whelan, M. Rossi, M. Morrison, G. Holtmann and J. T. Kelly, *et al.*, Dietary fiber intervention on gut microbiota composition in healthy adults: a systematic review and meta-analysis, *Am. J. Clin. Nutr.*, 2018, **107**(6), 965–983, DOI: **10.1093/ajcn/nqy041**.

4 F. Bishehsari, P. A. Engen, N. Z. Preite, Y. E. Tuncil, A. Naqib and M. Shaikh, *et al.*, Dietary Fiber Treatment Corrects the Composition of Gut Microbiota, Promotes SCFA Production, and Suppresses Colon Carcinogenesis, *Genes*, 2018, **9**(2), 102, DOI: **10.3390/genes9020102**.

5 K. Makki, E. C. Deehan, J. Walter and F. Bäckhed, The Impact of Dietary Fiber on Gut Microbiota in Host Health and Disease, *Cell Host Microbe*, 2018, **23**(6), 705–715, DOI: **10.1016/j.chom.2018.05.012**.

6 X. Wu, Y. Wu, L. He, L. Wu, X. Wang and Z. Liu, Effects of the intestinal microbial metabolite butyrate on the development of colorectal cancer, *J. Cancer*, 2018, **9**(14), 2510–2517, DOI: **10.7150/jca.25324**.

7 M. Waldecker, T. Kautenburger, H. Daumann, C. Busch and D. Schrenk, Inhibition of histone-deacetylase activity by short-chain fatty acids and some polyphenol metabolites formed in the colon, *J. Nutr. Biochem.*, 2008, **19**(9), 587–593, DOI: **10.1016/j.jnutbio.2007.08.002**.

8 M. Sahuri-Arisoylu, R. R. Mould, N. Shinjyo, S. W. A. Bligh, A. V. W. Nunn and G. W. Guy, *et al.*, Acetate Induces Growth Arrest in Colon Cancer Cells Through Modulation of Mitochondrial Function, *Front. Nutr.*, 2021, **8**, 588466, DOI: **10.3389/fnut.2021.588466**.

9 C. S. F. Oliveira, H. Pereira, S. Alves, L. Castro, F. Baltazar and S. R. Chaves, *et al.*, Cathepsin D protects colorectal cancer cells from acetate-induced apoptosis through autophagy-independent degradation of damaged mitochondria, *Cell Death Dis.*, 2015, **6**(6), e1788, DOI: **10.1038/cddis.2015.157**.

10 C. Marques, C. S. F. Oliveira, S. Alves, S. R. Chaves, O. P. Coutinho and M. Côrte-Real, *et al.*, Acetate-induced apoptosis in colorectal carcinoma cells involves lysosomal membrane permeabilization and cathepsin D release, *Cell Death Dis.*, 2013, **4**(2), e507, DOI: **10.1038/cddis.2013.29**.

11 T. Y. Ryu, K. Kim, M.-Y. Son, J.-K. Min, J. Kim and T.-S. Han, *et al.*, Downregulation of PRMT1, a histone arginine methyltransferase, by sodium propionate induces cell apoptosis in colon cancer, *Oncol. Rep.*, 2019, **41**(3), 1691–1699, DOI: **10.3892/or.2018.6938**.

12 M.-T. Liong, Roles of Probiotics and Prebiotics in Colon Cancer Prevention: Postulated Mechanisms and In-vivo

Evidence, *Int. J. Mol. Sci.*, 2008, **9**(5), 854–863, DOI: **10.3390/ijms9050854**, PMID: 19325789.

13 J. Li, D. Chen and M. Shen, Tumor Microenvironment Shapes Colorectal Cancer Progression, Metastasis, and Treatment Responses, *Front. Med.*, 2022, **9**, 869010, DOI: **10.3389/fmed.2022.869010**.

14 H. H. van Ravenswaay Claasen, P. M. Kluin and G. J. Fleuren, Tumor infiltrating cells in human cancer. On the possible role of CD16+ macrophages in antitumor cytotoxicity, *Lab. Invest.*, 1992, **67**(2), 166–174.

15 W. H. McBride, Phenotype and functions of intratumoral macrophages, *Biochim. Biophys. Acta - Rev. Cancer*, 1986, **865**(1), 27–41, DOI: **10.1016/0304-419X(86)90011-9**.

16 L. Luput, E. Licarete, A. Sesarman, L. Patras, M. C. Alupei and M. Banciu, Tumor-associated macrophages favor C26 murine colon carcinoma cell proliferation in an oxidative stress-dependent manner, *Oncol. Rep.*, 2017, **37**(4), 2472–2480, DOI: **10.3892/or.2017.5466**.

17 H. Miao, J. Ou, Y. Peng, X. Zhang, Y. Chen and L. Hao, *et al.*, Macrophage ABHD5 promotes colorectal cancer growth by suppressing spermidine production by SRM, *Nat. Commun.*, 2016, **7**, 11716, DOI: **10.1038/ncomms11716**.

18 J. Lan, L. Sun, F. Xu, L. Liu, F. Hu and D. Song, *et al.*, M2 Macrophage-Derived Exosomes Promote Cell Migration and Invasion in Colon Cancer, *Cancer Res.*, 2019, **79**(1), 146–158, DOI: **10.1158/0008-5472.CAN-18-0014**.

19 A. Jedinak, S. Dudhgaonkar and D. Sliva, Activated macrophages induce metastatic behavior of colon cancer cells, *Immunobiology*, 2010, **215**(3), 242–249, DOI: **10.1016/j.imbio.2009.03.004**.

20 K. Vinnakota, Y. Zhang, B. C. Selvanesan, G. Topi, T. Salim and J. Sand-Dejmek, *et al.*, M2-like macrophages induce colon cancer cell invasion via matrix metalloproteinases, *J. Cell. Physiol.*, 2017, **232**(12), 3468–3480, DOI: **10.1002/jcp.25808**.

21 X. Wang and Y. Lin, Tumor necrosis factor and cancer, buddies or foes?, *Acta Pharmacol. Sin.*, 2008, **29**(11), 1275–1288, DOI: **10.1111/j.1745-7254.2008.00889.x**.

22 M. de Looff, S. de Jong and F. A. E. Kruyt, Multiple Interactions Between Cancer Cells and the Tumor Microenvironment Modulate TRAIL Signaling: Implications for TRAIL Receptor Targeted Therapy, *Front. Immunol.*, 2019, **10**, 1530, DOI: **10.3389/fimmu.2019.01530**.

23 M. Baay, A. Brouwer, P. Pauwels, M. Peeters and F. Lardon, Tumor Cells and Tumor-Associated Macrophages: Secreted Proteins as Potential Targets for Therapy, *Clin. Dev. Immunol.*, 2011, **2011**, 565187, DOI: **10.1155/2011/565187**.

24 C. Han, C. Zhang, H. Wang and L. Zhao, Exosome-mediated communication between tumor cells and tumor-associated macrophages: implications for tumor microenvironment, *Onco Targets Ther*, 2021, **10**(1), 1887552, DOI: **10.1080/2162402X.2021.1887552**.

25 Q. Chen, S. Nair and C. Ruedl, Microbiota regulates the turnover kinetics of gut macrophages in health and inflammation, *Life Sci. Alliance*, 2022, **5**(1), e202101178, DOI: **10.26508/lsa.202101178**.

26 S. Mola, C. Pandolfo, A. Sica and C. Porta, The Macrophages-Microbiota Interplay in Colorectal Cancer (CRC)-Related Inflammation: Prognostic and Therapeutic Significance, *Int. J. Mol. Sci.*, 2020, **21**(18), 6866, DOI: **10.3390/ijms21186866**.

27 H. Fang, R. A. Pengal, X. Cao, L. P. Ganesan, M. D. Wewers and C. B. Marsh, *et al.*, Lipopolysaccharide-induced macrophage inflammatory response is regulated by SHIP, *J. Immunol.*, 2004, **173**(1), 360–366, DOI: **10.4049/jimmunol.173.1.360**.

28 J. Ji, D. Shu, M. Zheng, J. Wang, C. Luo and Y. Wang, *et al.*, Microbial metabolite butyrate facilitates M2 macrophage polarization and function, *Sci. Rep.*, 2016, **6**(1), 1–10, DOI: **10.1038/srep24838**.

29 J. Schulthess, S. Pandey, M. Capitani, K. C. Rue-Albrecht, I. Arnold and F. Franchini, *et al.*, The Short Chain Fatty Acid Butyrate Imprints an Antimicrobial Program in Macrophages, *Immunity*, 2019, **50**(2), 432–445.e7, DOI: **10.1016/j.immuni.2018.12.018**.

30 C. Pleguezuelos-Manzano, J. Puschhof, A. Rosendahl Huber, A. van Hoeck, H. M. Wood and J. Nomburg, *et al.*, Mutational signature in colorectal cancer caused by genotoxic pks+ E. coli, *Nature*, 2020, **580**(7802), 269–273, DOI: **10.1038/s41586-020-2080-8**.

31 H. J. Kim, H. Li, J. J. Collins and D. E. Ingber, Contributions of microbiome and mechanical deformation to intestinal bacterial overgrowth and inflammation in a human gut-on-a-chip, *Proc. Natl. Acad. Sci. U. S. A.*, 2016, **113**(1), E7–E15, DOI: **10.1073/pnas.1522193112**.

32 K. Greenhalgh, J. Ramiro-Garcia, A. Heinken, P. Ullmann, T. Bintener and M. P. Pacheco, *et al.*, Integrated In Vitro and In Silico Modeling Delineates the Molecular Effects of a Synbiotic Regimen on Colorectal-Cancer-Derived Cells, *Cell Rep.*, 2019, **27**(5), 1621–1632.e9, DOI: **10.1016/j.celrep.2019.04.001**.

33 D. Penarete-Acosta, R. Stading, L. Emerson, M. Horn, S. Chakraborty and A. Han, *et al.*, A microfluidic co-culture model for investigating colonocytes–microbiota interactions in colorectal cancer, *Lab Chip*, 2024, **24**(15), 3690–3703, DOI: **10.1039/D4LC00013G**.

34 E. K. Park, H. S. Jung, H. I. Yang, M. C. Yoo, C. Kim and K. S. Kim, Optimized THP-1 differentiation is required for the detection of responses to weak stimuli, *Inflammation Res.*, 2007, **56**(1), 45–50, DOI: **10.1007/s00011-007-6115-5**.

35 T. Starr, T. J. Bauler, P. Malik-Kale and O. Steele-Mortimer, The phorbol 12-myristate-13-acetate differentiation protocol is critical to the interaction of THP-1 macrophages with Salmonella Typhimurium, *PLoS One*, 2018, **13**(3), e0193601, DOI: **10.1371/journal.pone.0193601**.

36 M. E. Lund, J. To, B. A. O'Brien and S. Donnelly, The choice of phorbol 12-myristate 13-acetate differentiation protocol influences the response of THP-1 macrophages to a pro-inflammatory stimulus, *J. Immunol. Methods*, 2016, **430**, 64–70, DOI: **10.1016/j.jim.2016.01.012**.

37 Y. Ma, M. Hu, L. Zhou, S. Ling, Y. Li and B. Kong, *et al.*, Dietary fiber intake and risks of proximal and distal colon cancers: A meta-analysis, *Medicine*, 2018, **97**(36), e11678, DOI: **10.1097/MD.0000000000011678**.

38 B. L. Pool-Zobel and J. Sauer, Overview of Experimental Data on Reduction of Colorectal Cancer Risk by Inulin-Type Fructans, *J. Nutr.*, 2007, **137**(11), 2580S–2584S, DOI: **10.1093/jn/137.11.2580S**.

39 J. H. Cummings, G. T. Macfarlane and H. N. Englyst, Prebiotic digestion and fermentation, *Am. J. Clin. Nutr.*, 2001, **73**(2), 415s–420s, DOI: **10.1093/ajcn/73.2.415s**.

40 J. Xiao, B. U. Metzler-Zebeli and Q. Zebeli, Gut Function-Enhancing Properties and Metabolic Effects of Dietary Indigestible Sugars in Rodents and Rabbits, *Nutrients*, 2015, **7**(10), 8348–8365, DOI: **10.3390/nu7105397**.

41 G. Falony, T. Calmeyn, F. Leroy and L. De Vuyst, Coculture Fermentations of Bifidobacterium Species and Bacteroides thetaiotaomicron Reveal a Mechanistic Insight into the Prebiotic Effect of Inulin-Type Fructans, *Appl. Environ. Microbiol.*, 2009, **75**(8), 2312–2319, DOI: **10.1128/AEM.02649-08**.

42 S. Hiel, M. A. Gianfrancesco, J. Rodriguez, D. Portheault, Q. Leyrolle and L. B. Bindels, *et al.*, Link between gut microbiota and health outcomes in inulin -treated obese patients: Lessons from the Food4Gut multicenter randomized placebo-controlled trial, *Clin. Nutr.*, 2020, **39**(12), 3618–3628, DOI: **10.1016/j.clnu.2020.04.005**.

43 D. Vandeputte, G. Falony, S. Vieira-Silva, J. Wang, M. Sailer and S. Theis, *et al.*, Prebiotic inulin-type fructans induce specific changes in the human gut microbiota, *Gut*, 2017, **66**(11), 1968–1974, DOI: **10.1136/gutjnl-2016-313271**.

44 Q. Le Bastard, G. Chapelet, F. Javaudin, D. Lepelletier, E. Batard and E. Montassier, The effects of inulin on gut microbial composition: a systematic review of evidence from human studies, *Eur. J. Clin. Microbiol. Infect. Dis.*, 2020, **39**(3), 403–413, DOI: **10.1007/s10096-019-03721-w**.

45 X. Wang, T. Wang, Q. Zhang, L. Xu and X. Xiao, Dietary Supplementation with Inulin Modulates the Gut Microbiota and Improves Insulin Sensitivity in Prediabetes, *Int. J. Endocrinol.*, 2021, **2021**, 5579369, DOI: **10.1155/2021/5579369**.

46 J. Fernández, E. Ledesma, J. Monte, E. Millán, P. Costa and V. G. de la Fuente, *et al.*, Traditional Processed Meat Products Re-designed Towards Inulin-rich Functional Foods Reduce Polyps in Two Colorectal Cancer Animal Models, *Sci. Rep.*, 2019, **9**(1), 14783, DOI: **10.1038/s41598-019-51437-w**.

47 C. V. Rao, D. Chou, B. Simi, H. Ku and B. S. Reddy, Prevention of colonic aberrant crypt foci and modulation of large bowel microbial activity by dietary coffee fiber, inulin and pectin, *Carcinogenesis*, 1998, **19**(10), 1815–1819, DOI: **10.1093/carcin/19.10.1815**.

48 M. Poulsen, A.-M. Mølck and B. L. Jacobsen, Different effects of short- and long-chained fructans on large intestinal physiology and carcinogen-induced aberrant crypt foci in rats, *Nutr. Cancer*, 2002, **42**(2), 194–205, DOI: **10.1207/S15327914NC422_8**.

49 A. P. Femia, C. Luceri, P. Dolara, A. Giannini, A. Biggeri and M. Salvadori, *et al.*, Antitumorigenic activity of the prebiotic inulin enriched with oligofructose in combination with the probiotics Lactobacillus rhamnosus and Bifidobacterium lactis on azoxymethane-induced colon carcinogenesis in rats, *Carcinogenesis*, 2002, **23**(11), 1953–1960, DOI: **10.1093/carcin/23.11.1953**.

50 Z. Wang, X. Zhang, L. Zhu, X. Yang, F. He and T. Wang, *et al.*, Inulin alleviates inflammation of alcoholic liver disease via SCFAs-inducing suppression of M1 and facilitation of M2 macrophages in mice, *Int. Immunopharmacol.*, 2019, **78**, 106062, DOI: **10.1016/j.intimp.2019.106062**.

51 H. Nakajima, N. Nakanishi, T. Miyoshi, T. Okamura, Y. Hashimoto and T. Senmaru, *et al.*, Inulin reduces visceral adipose tissue mass and improves glucose tolerance through altering gut metabolites, *Nutr. Metab.*, 2022, **19**(1), 50, DOI: **10.1186/s12986-022-00685-1**.

52 D. Rios-Covian, N. Salazar, M. Gueimonde and C. G. de los Reyes-Gavilan, Shaping the Metabolism of Intestinal Bacteroides Population through Diet to Improve Human Health, *Front. Microbiol.*, 2017, **7**(8), 376.

53 P. Louis and H. J. Flint, Formation of propionate and butyrate by the human colonic microbiota, *Environ. Microbiol.*, 2017, **19**(1), 29–41, DOI: **10.1111/1462-2920.13589**.

54 F. De Mets, L. Van Melderen and S. Gottesman, Regulation of acetate metabolism and coordination with the TCA cycle via a processed small RNA, *Proc. Natl. Acad. Sci. U. S. A.*, 2019, **116**(3), 1043–1052, DOI: **10.1073/pnas.1815288116**.

55 H. L. Lee, H. Shen, I. Y. Hwang, H. Ling, W. S. Yew and Y. S. Lee, *et al.*, Targeted Approaches for In Situ Gut Microbiome Manipulation, *Genes*, 2018, **9**(7), 351, DOI: **10.3390/genes9070351**.

56 E. Birkeland, S. Gharagozlian, K. I. Birkeland, J. Valeur, I. Måge and I. Rud, *et al.*, Prebiotic effect of inulin-type fructans on faecal microbiota and short-chain fatty acids in type 2 diabetes: a randomised controlled trial, *Eur. J. Nutr.*, 2020, **59**(7), 3325–3338, DOI: **10.1007/s00394-020-02282-5**.

57 S. A. Poeker, C. Lacroix, T. de Wouters, M. R. Spalinger, M. Scharl and A. Geirnaert, Stepwise Development of an in vitro Continuous Fermentation Model for the Murine Caecal Microbiota, *Front. Microbiol.*, 2019, **29**(10), 1166, DOI: **10.3389/fmicb.2019.01166**.

58 Z. C. Holmes, M. M. Villa, H. K. Durand, S. Jiang, E. P. Dallow and B. L. Petrone, *et al.*, Microbiota responses to different prebiotics are conserved within individuals and associated with habitual fiber intake, *Microbiome*, 2022, **10**(1), 114, DOI: **10.1186/s40168-022-01307-x**.

59 D. R. Donohoe, D. Holley, L. B. Collins, S. A. Montgomery, A. C. Whitmore and A. Hillhouse, *et al.*, A Gnotobiotic Mouse Model Demonstrates that Dietary Fiber Protects Against Colorectal Tumorigenesis in a Microbiota- and Butyrate–Dependent Manner, *Cancer Discovery*, 2014, **4**(12), 1387–1397, DOI: **10.1158/2159-8290.CD-14-0501**.

60 R. Fan, K. Naqvi, K. Patel, J. Sun and J. Wan, Evaporation-based microfluidic production of oil-free cell-containing hydrogel particles, *Biomicrofluidics*, 2015, **9**(5), 052602, DOI: **10.1063/1.4916508**.

61 C. A. Wilson and J. L. Browning, Death of HT29 adenocarcinoma cells induced by TNF family receptor activation is caspase-independent and displays features of both apoptosis and necrosis, *Cell Death Differ.*, 2002, **9**(12), 1321–1333, DOI: **10.1038/sj.cdd.4401107**.

62 S. Eslick, E. J. Williams, B. S. Berthon, T. Wright, C. Karihaloo and M. Gately, *et al.*, Weight Loss and Short-Chain Fatty Acids Reduce Systemic Inflammation in Monocytes and Adipose Tissue Macrophages from Obese Subjects, *Nutrients*, 2022, **14**(4), 765, DOI: **10.3390/nu14040765**.

63 S. Gazzaniga, A. I. Bravo, A. Guglielmotti, N. van Rooijen, F. Maschi and A. Vecchi, *et al.*, Targeting Tumor-Associated Macrophages and Inhibition of MCP-1 Reduce Angiogenesis and Tumor Growth in a Human Melanoma Xenograft, *J. Invest. Dermatol.*, 2007, **127**(8), 2031–2041, DOI: **10.1038/sj.jid.5700827**.

64 K. Fousek, L. A. Horn and C. Palena, Interleukin-8: A chemokine at the intersection of cancer plasticity, angiogenesis, and immune suppression, *Pharmacol. Ther.*, 2021, **219**, 107692, DOI: **10.1016/j.pharmthera.2020.107692**.

65 R. Sun and C. Abraham, IL23 Promotes Antimicrobial Pathways in Human Macrophages, Which Are Reduced With the IBD-Protective IL23R R381Q Variant, *Cell. Mol. Gastroenterol. Hepatol.*, 2020, **10**(4), 673–697, DOI: **10.1016/j.jcmgh.2020.05.007**.

66 R. Sun, M. Hedl and C. Abraham, IL23 induces IL23R recycling and amplifies innate receptor-induced signalling and cytokines in human macrophages, and the IBD-protective IL23R R381Q variant modulates these outcomes, *Gut*, 2020, **69**(2), 264–273, DOI: **10.1136/gutjnl-2018-316830**.

67 D. Jorgovanovic, M. Song, L. Wang and Y. Zhang, Roles of IFN-γ in tumor progression and regression: a review, *Biomark. Res.*, 2020, **29**(8), 49, DOI: **10.1186/s40364-020-00228-x**.

68 K. R. B. Bastos, C. R. F. Marinho, R. Barboza, M. Russo, J. M. Álvarez and M. R. D'Império Lima, What kind of message does IL-12/IL-23 bring to macrophages and dendritic cells?, *Microbes Infect.*, 2004, **6**(6), 630–636, DOI: **10.1016/j.micinf.2004.02.012**.

69 A. Masztalerz, N. Van Rooijen, W. Den Otter and L. A. Everse, Mechanisms of macrophage cytotoxicity in IL-2 and IL-12 mediated tumour regression, *Cancer Immunol. Immunother.*, 2003, **52**(4), 235–242, DOI: **10.1007/s00262-003-0381-z**.

70 J. Yan, M. J. Smyth and M. W. L. Teng, Interleukin (IL)-12 and IL-23 and Their Conflicting Roles in Cancer, *Cold Spring Harbor Perspect. Biol.*, 2018, **10**(7), a028530, DOI: **10.1101/cshperspect.a028530**.

71 Inhibition of IL-8 Receptor Reduces Colorectal Cancer Proliferation - The ASCO Post [Internet]. [cited 2021 Jul 13], Available from: **https://ascopost.com/issues/may-15-2012/inhibition-of-il-8-receptor-reduces-colorectal-cancer-proliferation/**.

72 S. Krishnan, Y. Ding, N. Saedi, M. Choi, G. V. Sridharan and D. H. Sherr, *et al.*, Gut Microbiota-Derived Tryptophan Metabolites Modulate Inflammatory Response in Hepatocytes and Macrophages, *Cell Rep.*, 2018, **23**(4), 1099–1111, DOI: **10.1016/j.celrep.2018.03.109**.

73 S. J. D. O'Keefe, Diet, microorganisms and their metabolites, and colon cancer, *Nat. Rev. Gastroenterol. Hepatol.*, 2016, **13**(12), 691–706, DOI: **10.1038/nrgastro.2016.165**.

74 K. Y. C. Fung, G. V. Brierley, S. Henderson, P. Hoffmann, S. R. McColl and T. Lockett, *et al.*, Butyrate-induced apoptosis in HCT116 colorectal cancer cells includes induction of a cell stress response, *J. Proteome Res.*, 2011, **10**(4), 1860–1869, DOI: **10.1021/pr1011125**.

75 C. Ramirez-Farias, K. Slezak, Z. Fuller, A. Duncan, G. Holtrop and P. Louis, Effect of inulin on the human gut microbiota: stimulation of Bifidobacterium adolescentis and Faecalibacterium prausnitzii, *J. Geophys. Res.:Oceans*, 2008, **101**(4), 541–550, DOI: **10.1017/S0007114508019880**.

76 N. T. Baxter, A. W. Schmidt, A. Venkataraman, K. S. Kim, C. Waldron and T. M. Schmidt, Dynamics of Human Gut Microbiota and Short-Chain Fatty Acids in Response to Dietary Interventions with Three Fermentable Fibers, *MBio*, 2019, **10**(1), e02566-18, DOI: **10.1128/mBio.02566-18**.

77 N. Salazar, E. M. Dewulf, A. M. Neyrinck, L. B. Bindels, P. D. Cani and J. Mahillon, *et al.*, Inulin-type fructans modulate intestinal Bifidobacterium species populations and decrease fecal short-chain fatty acids in obese women, *Clin. Nutr.*, 2015, **34**(3), 501–507, DOI: **10.1016/j.clnu.2014.06.001**.

78 G. Healey, R. Murphy, C. Butts, L. Brough, K. Whelan and J. Coad, Habitual dietary fibre intake influences gut microbiota response to an inulin-type fructan prebiotic: a randomised, double-blind, placebo-controlled, cross-over, human intervention study, *J. Geophys. Res.:Oceans*, 2018, **119**(2), 176–189, DOI: **10.1017/S0007114517003440**.

79 F. Liu, P. Li, M. Chen, Y. Luo, M. Prabhakar and H. Zheng, *et al.*, Fructooligosaccharide (FOS) and Galactooligosaccharide (GOS) Increase Bifidobacterium but Reduce Butyrate Producing Bacteria with Adverse Glycemic Metabolism in healthy young population, *Sci. Rep.*, 2017, **7**(1), 11789, DOI: **10.1038/s41598-017-10722-2**.

80 H. D. Holscher, L. L. Bauer, V. Gourineni, C. L. Pelkman, G. C. Fahey Jr. and K. S. Swanson, Agave Inulin Supplementation Affects the Fecal Microbiota of Healthy Adults Participating in a Randomized, Double-Blind, Placebo-Controlled, Crossover Trial, *J. Nutr.*, 2015, **145**(9), 2025–2032, DOI: **10.3945/jn.115.217331**.

81 M. Roller, A. Pietro Femia, G. Caderni, G. Rechkemmer and B. Watzl, Intestinal immunity of rats with colon cancer is modulated by oligofructose-enriched inulin combined with Lactobacillus rhamnosus and Bifidobacterium lactis, *J. Geophys. Res.:Oceans*, 2004, **92**(6), 931–938, DOI: **10.1079/bjn20041289**.

82 Y. Li, L. Elmén, I. Segota, Y. Xian, R. Tinoco and Y. Feng, *et al.*, Prebiotic-Induced Anti-tumor Immunity Attenuates Tumor Growth, *Cell Rep.*, 2020, **30**(6), 1753–1766.e6, DOI: **10.1016/j.celrep.2020.01.035**.

83 R. Braster, M. Bögels, R. H. J. Beelen and M. van Egmond, The delicate balance of macrophages in colorectal cancer; their role in tumour development and therapeutic potential, *Immunobiology*, 2017, **222**(1), 21–30, DOI: **10.1016/j.imbio.2015.08.011**.

84 X. Zhong, B. Chen and Z. Yang, The Role of Tumor-Associated Macrophages in Colorectal Carcinoma Progression, *Cell. Physiol. Biochem.*, 2018, **45**(1), 356–365, DOI: **10.1159/000486816**.

85 J. Li, L. Li, Y. Li, Y. Long, Q. Zhao and Y. Ouyang, *et al.*, Tumor-associated macrophage infiltration and prognosis in colorectal cancer: systematic review and meta-analysis, *Int. J. Colorectal Dis.*, 2020, **35**(7), 1203–1210, DOI: **10.1007/s00384-020-03593-z**.

86 A. Bein, W. Shin, S. Jalili-Firoozinezhad, M. H. Park, A. Sontheimer-Phelps and A. Tovaglieri, *et al.*, Microfluidic Organ-on-a-Chip Models of Human Intestine, *Cell. Mol. Gastroenterol. Hepatol.*, 2018, **5**(4), 659–668, DOI: **10.1016/j.jcmgh.2017.12.010**.

87 G. Falony, K. Lazidou, A. Verschaeren, S. Weckx, D. Maes and L. De Vuyst, In Vitro Kinetic Analysis of Fermentation of Prebiotic Inulin-Type Fructans by Bifidobacterium Species Reveals Four Different Phenotypes, *Appl. Environ. Microbiol.*, 2009, **75**(2), 454–461, DOI: **10.1128/AEM.01488-08**.

88 M. J. Logtenberg, R. Akkerman, R. An, G. D. A. Hermes, B. J. de Haan and M. M. Faas, *et al.*, Fermentation of Chicory Fructo-Oligosaccharides and Native Inulin by Infant Fecal Microbiota Attenuates Pro-Inflammatory Responses in Immature Dendritic Cells in an Infant-Age-Dependent and Fructan-Specific Way, *Mol. Nutr. Food Res.*, 2020, **64**(13), 2000068, DOI: **10.1002/mnfr.202000068**.

89 N. Zhang, Z. Wang and Y. Zhao, Selective inhibition of Tumor necrosis factor receptor-1 (TNFR1) for the treatment of autoimmune diseases, *Cytokine Growth Factor Rev.*, 2020, **55**, 80–85, DOI: **10.1016/j.cytogfr.2020.03.002**.

90 S. Covarrubias, A. C. Vollmers, A. Capili, M. Boettcher, A. Shulkin and M. R. Correa, *et al.*, High-Throughput CRISPR Screening Identifies Genes Involved in Macrophage Viability and Inflammatory Pathways, *Cell Rep.*, 2020, **33**(13), 108541, DOI: **10.1016/j.celrep.2020.108541**.

91 S. Tedesco, F. De Majo, J. Kim, A. Trenti, L. Trevisi and G. P. Fadini, *et al.*, Convenience versus Biological Significance: Are PMA-Differentiated THP-1 Cells a Reliable Substitute for Blood-Derived Macrophages When Studying in Vitro Polarization?, *Front. Pharmacol.*, 2018, **9**, 71, DOI: **10.3389/fphar.2018.00071**.

92 A. Dhariwal, J. Chong, S. Habib, I. L. King, L. B. Agellon and J. Xia, MicrobiomeAnalyst: a web-based tool for comprehensive statistical, visual and meta-analysis of microbiome data, *Nucleic Acids Res.*, 2017, **45**(W1), W180–W188, DOI: **10.1093/nar/gkx295**.

93 S. Derveaux, J. Vandesompele and J. Hellemans, How to do successful gene expression analysis using real-time PCR, *Methods*, 2010, **50**(4), 227–230, DOI: **10.1016/j.ymeth.2009.11.001**.